

**OPTIMIZATION OF CONVERGENT ANGLE OF VENTURI  
METER FOR THE BEST COEFFICIENT OF DISCHARGE**

A DISSERTATION

SUBMITTED IN PARTIAL FULFILLMENT OF THE REQUIREMENTS

FOR THE AWARD OF THE DEGREE

OF

MASTER OF TECHNOLOGY

IN

**HYDRAULICS AND WATER RESOURCES ENGINEERING**

Submitted By:

**Naman Jain**

**2K17/HFE/11**

Under the supervision of

**Dr. S. ANBU KUMAR**



**CIVIL ENGINEERING DEPARTMENT**

**DELHI TECHNOLOGICAL UNIVERSITY**

(Formerly Delhi College of Engineering)

Bawana Road, Delhi-110042

July, 2019

**DELHI TECHNOLOGICAL UNIVERSITY****(Formerly Delhi College of Engineering)**

Bawana Road, Delhi-110042

**CANDIDATE'S DECLARATION**

I, Naman Jain, Roll No. 2K17/HFE/11 student of M.Tech. (Hydraulics and Water Resources Engineering), hereby declare that the project dissertation titled "Optimization of Convergent Angle of Venturi Meter for best Coefficient Of Discharge" which is submitted by me to the Department of Civil Engineering, Delhi Technological University, Delhi in partial fulfilment of the requirement for the award of the degree of Master of Technology, is original and not copied from any source without proper citation. This work has not previously formed the basis for the award of any Degree, Diploma Associate ship, Fellowship or other similar title of recognition.

Place: Delhi

**Naman Jain**

Date: 16/07/2019

2K17/HFE/11

(M.TECH)

**DEPARTMENT OF CIVIL ENGINEERING**  
**DELHI TECHNOLOGICAL UNIVERSITY**  
(Formerly Delhi College of Engineering)  
Bawana Road, Delhi-110042

**CERTIFICATE**

I hereby certify that the Project Dissertation titled “**OPTIMIZATION OF CONVERGENT ANGLE OF THE VENTURI METER FOR THE BEST COEFFICIENT OF DISCHARGE**” which is submitted by **Naman Jain**, 2K17/HFE/11, Department of Civil Engineering, Delhi Technological University, Delhi in partial fulfilment of the requirement for the award of the degree of Master of Technology, is a record of the project work carried out by the student under my supervision. To the best of my knowledge this work has not been submitted in part or full for any Degree or Diploma to this University or elsewhere.

Place: Delhi

Date: 25/07/2019

**Dr. S. Anbu Kumar**

SUPERVISOR

(Associate Professor)

DEPARTMENT OF CIVIL ENGINEERING

## ABSTRACT

Computational Fluid Dynamics is a compelling technique for getting stream flow and anticipating how this flow will react to various limiting boundary conditions. With this learning, the focal point of this research is to apply computational fluid elements such as CFD to issues dealing with stream flow measurement/estimation in closed conduits such as pipes utilizing differential stream meter like the Venturi meter. After thorough research from the existing literature it was determined that the Convergent Angle of a standard Venturi Meter has not been optimised in the existing studies. In simple words, there is a lack of literature pointing out that value of CA, for which the coefficient of discharge has the highest value or pressure differential between two Venturi sections is the least. This became the focus of present study.

The range given for a standard ASME Venturi CA is 20-22°. However, for the sake of experimentation the range of 19-22° is taken into consideration in this study. More than 50 models were created and run in ANSYS FLUENT, which was used as a CFD tool. Three  $\beta$  ratios are taken into consideration here, that are 0.4, 0.5 and 0.6. An optimum value of CA, corresponding to each  $\beta$  is found by finding out the best coefficient of discharge (closest to 0.99) for each test value of CA. Another aspect explored in this research is the relationship of Reynolds Number and Coefficient of Discharge. The effect of Reynolds Number on  $C_d$  is observed. This is done with the integration of ANSYS and laboratory results. The results of this study yields a definite value of CA for each  $\beta$  value. Along with this, a positive gradient followed by a Re vs  $C_d$  curve has been well established through Fluent. This is also validated by laboratory results.

## ACKNOWLEDGEMENT

I would like to express my sincere gratitude to my project supervisor, Dr. S. Anbu Kumar (Associate Professor, DTU), for his supervision, invaluable guidance, motivation and support throughout the extent of my project. I have been benefited immensely, from his wealth of knowledge. I would also like to extend a thankful note to Saurabh Sah (Phd Scholar, DTU) and Zohaib Ahmed Khan (M.Tech student, DTU) for helping me at different steps in this project. I extend my gratitude to my college, Delhi Technological University (formerly Delhi College of Engineering) for giving me the opportunity to carry out this project. I would also like to thank Dr. Nirendra Dev (Head of Department, Department of Civil Engineering, DTU) for making available all the necessary facilities that were required for my project.

This opportunity will be a significant milestone in my career development. I will strive to use the gained skills and knowledge in the best possible way, and I will continue to work on their improvement, in order to attain desired career objectives.

Date:

Place:

Naman Jain

# CONTENTS

	<b>PAGE NO.</b>
<b>Candidate Declaration</b>	<b>(ii)</b>
<b>Certificate</b>	<b>(iii)</b>
<b>Abstract</b>	<b>(iv)</b>
<b>Acknowledgement</b>	<b>(v)</b>
<b>List of Tables</b>	<b>(viii)</b>
<b>List of Figures</b>	<b>(ix)</b>
<b>List of Abbreviations</b>	<b>(xi)</b>
<b>CHAPTER 1 INTRODUCTION</b>	<b>1</b>
1.1 Venturimeter	1
1.1.1 Construction of Venturimeter	2
1.1.1.1 Convergent Inlet Cone	2
1.1.1.2 Throat Section	3
1.1.1.3 Divergent/ Recovery Cone Section	3
1.1.2 Functioning Of Venturimeter	4
1.1.2.1 Assumptions for Bernoulli's	5
1.2 Fluent	7
1.2.1 Computational Fluid Dynamics	7
1.2.2 Reasons for using Ansys Fluent	8
1.3 Reynolds Number	8
1.4 Objective of the current study	10

<b>CHAPTER 2 REVIEW OF LITERATURE</b>	<b>11</b>
<b>CHAPTER 3 METHODOLOGY</b>	<b>18</b>
3.1 Procedure: Ansys Fluent	18
3.2 Procedure: Lab	21
<b>CHAPTER 4 RESULTS</b>	<b>18</b>
4.1 Ansys Fluent Results	22
4.1.1 $\beta$ – ratio = 0.4	24
4.1.2 $\beta$ – ratio = 0.5	28
4.1.3 $\beta$ – ratio = 0.6	34
<b>CHAPTER 5 CONCLUSION</b>	<b>36</b>
<b>REFERENCES</b>	<b>39</b>

## List of Tables

<b>Table No</b>	<b>Description</b>	<b>Page No.</b>
Table 4.1	Theoretical discharge at different velocities	24
Table 4.1	$C_d$ for different converging angles of $\beta$ ratio = 0.4	25
Table 4.2	$C_d$ for different Reynolds Number for $\beta = 0.4$	26
Table 4.3	$C_d$ for different converging angles of $\beta$ ratio = 0.5	28
Table 4.4	$C_d$ for different Reynolds Number for $\beta = 0.5$	29
Table 4.5	$C_d$ for different converging angles of $\beta$ ratio = 0.6	31
Table 4.6	$C_d$ for different Reynolds Number for $\beta = 0.6$	32
Table 4.7	Experimental results for $\beta = 0.6$	34
Table 5.1	loss in pressure for different $\beta$ -ratios	36
Table 5.2	Optimum CA corresponding to different $\beta$ ratio	37
Table 5.3	Validation of the CFD results	37



## List of Figures

<b>Figure No.</b>	<b>Description</b>	<b>Page No.</b>
Figure 1.1	Basic model of Venturi meter	2
Figure 1.2	Venturi meter depicting two sections under consideration	4
Figure 1.3	Figure showing geometries with different convergent cone angles	9
Figure 1.4	A typical Venturi meter plane showing velocity contours.	9
Figure 1.5	Flow types	10
Figure 1.6	Idealised $Re$ vs $C_d$ curve	11
Figure 3.1	Geometry in SCDM	19
Figure 3.2	Figure depicting nodes and elements in a mesh	19
Figure 3.3	A surface plane depicting static pressure contour	21
Figure 3.2	Laboratory arrangement for the two Venturi meters	22
Figure 3.3	Collection tank of the Venturi meter	22
Figure 4.1	Pressure at two pressure taps	24
Figure 4.2	Graph showing the optimum Convergent angle for $\beta = 0.4$	25
Figure 4.3	Graphical representation of coefficient of discharge for different Reynolds Number and Convergent Angle for $\beta = 0.40$	27
Figure 4.4	Graph showing the optimum Convergent angle for $\beta = 0.5$	28

Figure 4.5	Graphical representation of coefficient of discharge for different Reynolds Number and Convergent Angle for $\beta = 0.5$	30
Figure 4.6	Graph showing the optimum Convergent angle for $\beta = 0.6$	31
Figure 4.7	Graphical representation of coefficient of discharge for different Reynolds Number and Convergent Angle for $\beta = 0.6$	33
Figure 4.8	Plot comparing lab and CFD results	35

**LIST OF ABBREVIATIONS**

ASME	American Society for Mechanical Engineers
SCDM	Space Claim Design Modeller
$\beta$ ratio	Diameter ratio
CA	Convergent Angle of Venturi Meter
u/s	Upstream
RCA	Recovery Cone Angle/Divergent Angle
$C_d$	Coefficient of Discharge
CFD	Computational Fluid Dynamics
PDE's	Partial Differential Equations
Re	Reynolds Number
b/w	between
FEA	Finite Element Analysis
$Q_{act}$	Actual Discharge
TB	Terabyte
ROM	Read Only Memory (Hard disk)
$Q_{theo}$	Theoretical Discharge

## CHAPTER 1

### INTRODUCTION

Precise measurement of fluid flow remains as one of the biggest concerns in many industries, because variations in flow measurement of the products costs these organisations considerable profits. With the increase in demand for highly accurate flow measurement meters, the use and application of Venturi Meters has increased many folds. In general, there are different meters used for computation of the flow of fluid: the Turbine-type meter, Rotameter, Orifice meter, and the Venturi meters are only a few. These meters work on their ability to alter/affect a certain physical property of the fluid flowing. The altered value of that property is then measured accurately. The measured change in that physical property is related to the flow then. For example, the physical property being pressure drop in Orifice and Venturi Meters. However, differential pressure flow meters of different types along with computer simulations are prevalent as well as more efficient techniques to compute flow measurement.

#### 1.1 VENTURIMETER

A Venturimeter, which is a differential pressure meter, is a measuring device which is used to compute the flow of fluids in a pipe. Likewise, a Venturi meter can be utilized for increment of the velocity of a liquid in pipes at a specific points. Bernoulli's Theorem remains as its working principle. The pressure of a moving fluid through a small cross section drops suddenly resulting in an increase in the flow velocity. The fluid which is initially having the characteristic of high pressure & low velocity will convert to low pressure and high velocity at a specific point and then again while approaching towards the Venturi outlet reaches to high pressure and low velocity. The point where Venturi meter is used, becomes the point of high velocity and low pressure. The latest Venturi model, Fig 1.1, comprises of a nozzle entrance as in ISA 1932 and a cone like development of convergent angle (also known as entry angle) no more noteworthy than

22°. The Venturi is expected to work in a tight Reynolds-number scope of  $1.5 \times 10^4$  to  $2 \times 10^6$ . It is known that Discharge Co-efficient ( $C_d$ ) is generally 0.95-0.99 for Venturi meter.

### 1.1.1. Construction of a Venturi meter

Venturi meter has a very basic construction. The standard Venturi meter has the below mentioned parts, arranged in a systematic matter for correct working. These are:

- Converging Cone also known as Inlet Section.
- Throat section or the cylindrical throat, and
- Diverging Cone or Recovery Cone

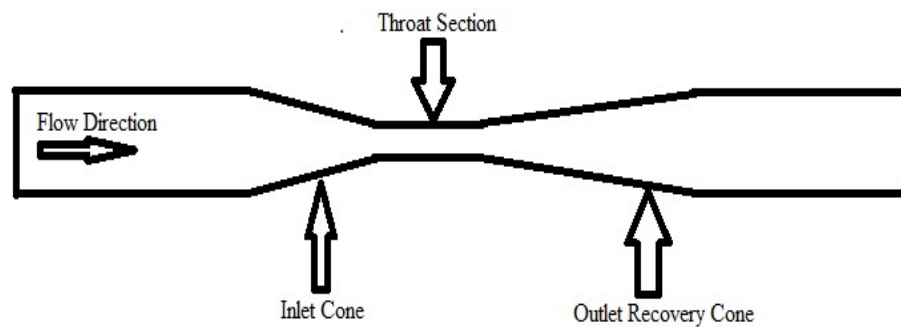


Figure 1.4 Basic model of Venturi meter

#### 1.1.1.1 Convergent Inlet Cone

Converging part is that region where the cross-section reduces to conical shape for the connection with the upstream pipe and its area of cross-section decreases from start to end. One of the inlet's end is connected to pipe at inlet which has a diameter of 30mm in this study whereas the other end is joined to the throat region whose diameter depends on the chosen  $\beta$  ratio. As per the ASME manual, 20-22 degree is generally the range of convergent angle whereas the length is kept as  $2.7(D-d)$ . In this expression, 'd' is the dia. of throat and D is the dia. of inlet section. The converging end, as mentioned above is attached to the cylindrical throat region at the downstream end. The decrement in the area of cross-section results in the fluid acceleration and decrease of static pressure. The maximum value of CA of the converging area is limited to prevent the Vena Contracta so the area of flow will be least at the throat. The convergent angle is believed

to be a function of  $\beta$  – ratio, as well as the Reynolds Number. Any change in Re or the  $\beta$ -ratio affects the most efficient convergent angle for that specific Venturi. A Venturi meters accuracy for the measurement of flow rate/discharge is very well documented and even established through various researches, however the part including design of convergent angles and the head loss associated with it isn't. This is the area under study in the current research.

#### 1.1.1.2 Throat Section

The Venturi meter has a central part called as throat which has the least area of cross-section. Length of this component is generally equal to its diameter. As per ASME, the range for dia. of throat lies in the range of 0.25 -0.75 times the dia. of the pipe at inlet, but mostly it is 0.5 of the dia. of the inlet pipe diameter. This term that is the ratio of throat diameter to the dia. of pipe at inlet, is often termed as the  $\beta$  ratio. The  $\beta$ -ratio acts as a very important physical parameter in designing a Venturi Meter. Throughout its length, the diameter of the throat remains unchanged. The diameter of throat cannot be reduced to its minimum suitable value because if cross sectional area decreases, velocity increases and pressure decreases. If this decrease for the value of pressure in any case goes below the vapour pressure of the fluid flowing through the Venturimeter, this can lead to cavitation. A limited diameter value is preferred in order to prevent this defect.

#### 1.1.1.3. Divergent/ Recovery Cone Section

The recovery Cone is the last component for this instrument. On one side, it is attached to the throat cylinder and the other to the pipe at outlet. The dia. of this section is increases gradually. As per the manual from ASME, the recovery cone has an angle of 5 to 13 degrees. The diverging angle is less than the converging angle due to which the length of the diverging cone is larger than converging cone. The primary reason for using a small angle of divergence is to avoid any flow separation from the walls and prevent the eddy formation. That is because the flow separation and eddies formation will results in large amount of loss in energy. In order to avoid these losses a proper angle of convergence and divergence is ensured. The divergent cone is often termed as recovery cone because it recovers the loss in pressure and also brings the velocity back to the normal value.

### 1.1.2 Functioning of Venturi meter

The working of Venturi meter can be described into following points:

- Bernoulli's principle as pointed earlier is the basis of the working of Venturi meter. On increase of velocity, the pressure decreases.
- At the convergent bit of the meter, as the area and pressure diminishes and there is a increment in velocity.
- Parameters such as pressure, area and velocity remain unaffected whereas the pressure gradient is zero in the cylindrical throat region. [that is  $(dp/dx) = 0$ ].
- Pressure drop b/w the inlet pipe and the throat region is measured with the help of manometer which is a differential type.
- Bernoulli's equation is used to calculate the discharge of fluid by the difference in height of the mercury column in the differential manometer.
- The reverse flow is eradicated as the angle of diverging section is restricted to a certain value. Pressure gradient observed here is adverse [i.e.,  $(dp/dx > 0)$ ].

One Venturi meter fitted in a horizontal pipe as shown in the Figure 1.2 is considered. Water flowing through the horizontal pipe is assumed. Two sections i.e. section 1 and section 2 as shown here in the figure 1.2 below are considered.

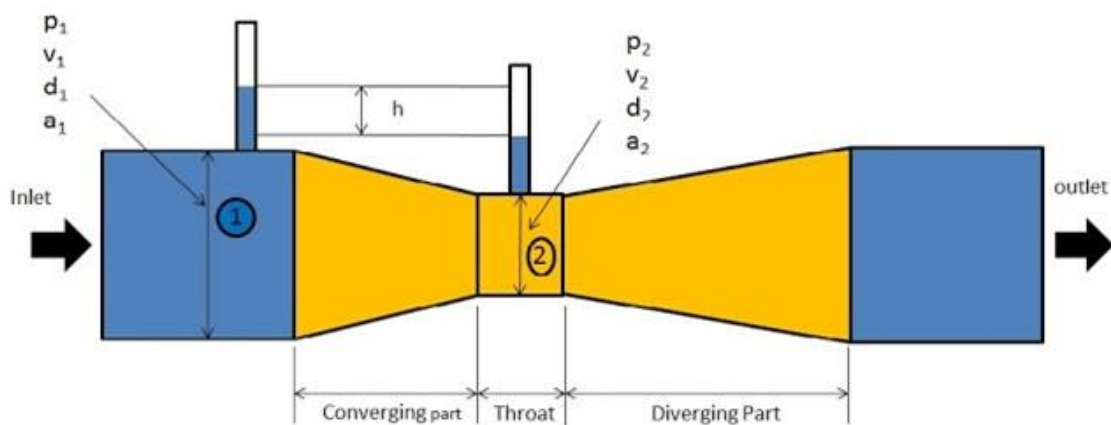


Figure 1.2 Venturi meter depicting two sections under consideration

$d_1$  = Diameter at section 1 (Inlet section)

$P_1$  = Pressure at section 1 (Inlet section)

$v_1$  = Velocity of fluid at section 1 (Inlet section)

$a_1$  = Area at section 1 (Inlet section) =  $(\pi/4) \times d_1^2$

$d_2$  = Diameter at section 2

$P_2$  = Pressure at section 2

$v_2$  = Velocity of fluid at section 2

$a_2$  = Area at section 2 =  $(\pi/4) \times d_2^2$

The Bernoulli's equation is applied at section 1 & section 2.

As per the Bernoulli's theorem, "in an incompressible, ideal fluid when the flow is steady and continuous, the sum of pressure energy, kinetic energy and potential energy will be constant along a stream line".

### 1.1.2.1 Assumptions for Bernoulli's

The Assumptions that are made for deriving Bernoulli's equation from Euler's equation of motion are as explained below.

1. Fluid considered for computation is ideal, i.e. In-viscid and incompressible.
2. The fluid that is flowing through is steady and continuous.
3. It is assumed that the flow of fluid is Irrotational.
4. Inner surface under consideration is taken as Frictionless.

On applying Bernoulli's equation at sections named as 1 & 2, the equations mentioned below are obtained :

$$\frac{p_1}{\rho g} + \frac{v_1^2}{2g} + z_1 = \frac{p_2}{\rho g} + \frac{v_2^2}{2g} + z_2$$

As the datum level remains the same:  $z_1 = z_2$

$$\frac{p_1}{\rho g} + \frac{v_1^2}{2g} = \frac{p_2}{\rho g} + \frac{v_2^2}{2g}$$

$$\frac{p_1 - p_2}{\rho g} = \frac{v_2^2 - v_1^2}{2g}$$

$$h = \frac{v_2^2 - v_1^2}{2g}$$

Here 'h' is given as the difference between pressure heads of two sections

The equation of continuity on the other hand gives :



$$a_1 * v_1 = a_2 * v_2$$

From this, it can be written that:

$$v_1 = \frac{a_2 * v_2}{a_1}$$

The above value of  $v_1$  in the above equation is substituted :

$$v_2 = \frac{a_1}{\sqrt{a_1^2 - a_2^2}} \sqrt{2gh}$$

With the help of this equation, determining the flow rate becomes easier now.

$$Q = a_2 * v_2$$

$$Q = \frac{a_1 a_2}{\sqrt{a_1^2 - a_2^2}} \sqrt{2gh}$$

The equation obtained above is known as the equation for theoretical discharge ( $Q_{th}$ ).

Actual discharge ( $Q_{act}$ ) will be less than the theoretical discharge . The reasons for which remain as the major and minor losses in the pipes

$$Q_{th} = \frac{a_1 a_2}{\sqrt{a_1^2 - a_2^2}} \sqrt{2gh}$$

$$Q_{act} = C_d \frac{a_1 a_2}{\sqrt{a_1^2 - a_2^2}} \sqrt{2gh} \quad (1.1)$$

$C_d$  is known as the “coefficient of discharge” and its value is supposed to be less than 1.

From the above equation,  $C_d$  can also be given as:

$$C_d = \frac{Q_{th}}{Q_{act}} \quad (1.2)$$

A typical value for  $C_d$  of an orifice meter is between 0.58 and 0.65, for a typical flow nozzle is between 0.93 and 0.98 and for the Venturi Meter is ranging from 0.95 to as high as 0.995. Venturi Meter therefore acts as one of the most efficient flow measuring devices, where the pressure losses are as less as 10 percent of the total pressure.

## 1.2 ANSYS FLUENT

The software package used in this study is ANSYS FLUENT. ANSYS, often known as Analysis System is a software package that is wide renowned for its Engineering Simulations. Fluent, which is an ANSYS solver containing wide physical abilities needed to model the flow, heat transfer, turbulence and reactions for different industrial applications. These range from flow of air over an aircraft wing to combustion occurring in a furnace, from structural analysis to oil platforms, from blood flow to flow in closed conduits and from clean room design to wastewater treatment plants . It is based on Computational Fluid Dynamics (CFD). Fluent spans over a huge range, including special models, with capabilities to model in-cylinder combustion, aero-acoustics, turbo machinery and multiphase systems. ANSYS FLUENT solution can be simulated for phenomenon of wide ranges: aerodynamic, hydrodynamic, mixture of liquid/gas, dispersion of particles, reacting flow, heat transfer, and much more. Even phenomena like steady state and transient flows can be very effectively solved.

### 1.2.1 Computational Fluid Dynamics

Computational fluid dynamics (CFD) is a way of using applied mathematics, physics and computational software to visualize how a fluid flows as well as how the gas or liquid affects objects as it flows past them .CFD has the Navier-Stokes equations as its basis. These equations give a description of how the pressure, velocity, temperature, and density of a moving fluid are related.

As said earlier, the very foundation of CFD is built on the Navier-Stokes equations, which are a set of partial differential equations (PDE's) that describe the flow of fluid. With CFD, the area of interest is sub-divided into a large number control volumes which can also be called as the cells. In each of these cells, the Navier-Stokes PDE's can be rewritten in the form of algebraic equations that relate the temperature, velocity, Flow rate, pressure, and other variables, such as species concentrations, to the values of these parameters in the neighbouring cells. Numerical simulation can be then used to solve these equations, yielding a complete picture of the flow domain, down to the resolution

of the grid. By solving the resulting set of equations iteratively, a complete description of the flow throughout the domain is yielded.

CFD provides information about the essential flow characteristics such as loss of pressure, distribution of flow, velocity contouring and mixing rates by solving the very fundamental equations governing the processes of fluid flow. Computational Fluid analysis is said to complement the traditional testing method and experimentation, thereby supplying an added insight and confidence in our designs. This leads to efficient designs, lower risk, and lesser time to the marketplace for different products or processes. Because of its ability and the ease of that ability to predict the performance of new designs or processes before they are produced or implemented, CFD has gradually become an integral part of the engineering analysis and design for many organisations. More importantly, the CFD software can result in fewer iterations to the final design, shorter lead times, and fewer expensive prototypes to manufacture. A cost-effective means for trying and testing model designs that would be too uneconomical and risky to investigate otherwise is enabled by CFD. Thereby, it can also be said that CFD also encourages innovation.

### 1.2.2 Reason for using ANSYS Fluent

- Turbulence Modelling: ANSYS Fluent software places a special emphasis on giving a wide range of turbulence models to capture the effects of kinetic energy and dissipation accurately and efficiently.  $k$ -epsilon,  $k$ - $\gamma$ ,  $\gamma$  - $\theta$  laminar-turbulent transition model are few innovative models which are available exclusively in ANSYS Fluent.
- The ease with which, incrementing / changing the angle and location of the convergent cone is possible.
- The ease by which the extraction of data at any location in the numerical domain from each modelling run can be done by plotting velocity/pressure contours.

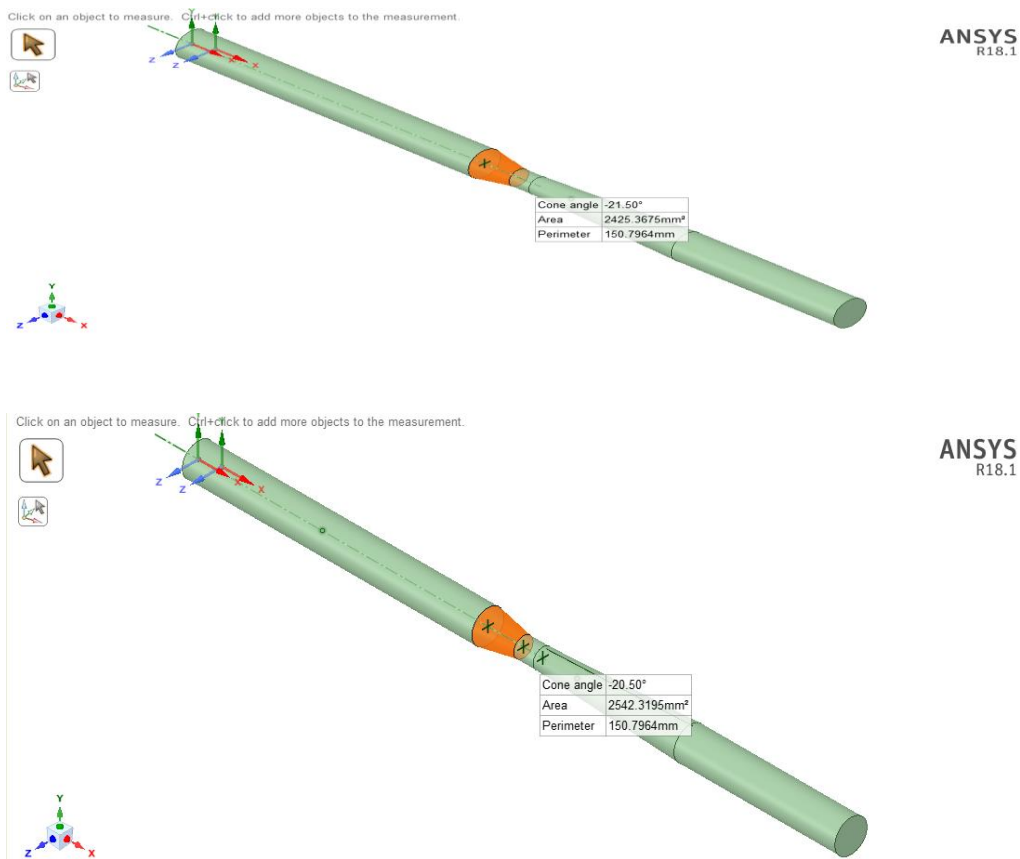


Figure 1.3 Figure showing geometries with different convergent cone angles

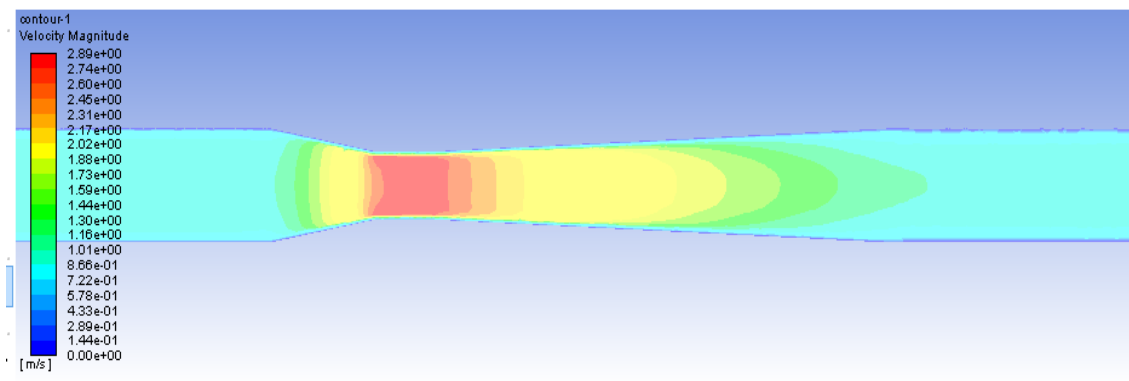


Figure 1.4 A typical Venturi meter plane showing velocity contours.

### 1.3 REYNOLDS NUMBER

Reynolds' number is a dimensionless physical quantity that is utilized to decide if the kind of stream flow as laminar, transient or turbulent while coursing through a pipe. Reynolds Number is characterized by the proportion of inertial force to that of viscous force. On the off chance that the Reynolds' number determined is high (more prominent than 2000), at that point the fluid motion through the pipe is said to be turbulent. In the event that Reynolds' no. is low (under 2000), the stream is said to be laminar. If the Reynolds no. values lie within the limit of 2,000 to 4,000, the flow is said to be in transition. Re is given by:

$$Re = \frac{\rho V D}{\mu} \quad (1.3)$$

Re = Reynolds's number

$\rho$  = the density of the fluid

V = velocity of flow

D = pipe diameter

$\mu$  = Dynamic viscosity of the fluid

Laminar stream is the sort of stream wherein the liquid voyages easily in ordinary ways through regular layered paths. Alternately, turbulent stream is not smooth and pursues an irregular path along-with loads of blending.

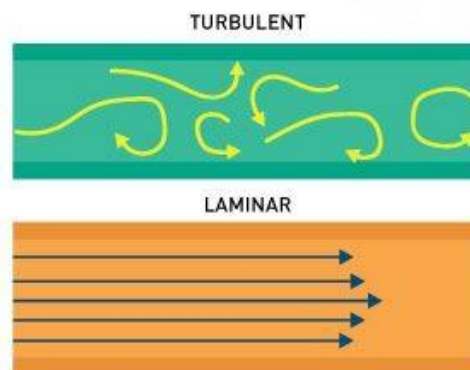


Figure 1.5 Flow types

The Reynolds Number plays important role when it comes to the pipe flows. In this study the effect of Reynolds number on the coefficient of discharge for the Venturi meter is studied. It is said that in the "turbulent" flows the fluid viscosity is less significant as compared to the laminar case and the velocity profile takes on a much more uniform shape. A range of turbulent Reynolds number has been studied here and the results are compared to come out to a conclusion.

Figure 1.6 gives an idealised curve for Reynolds Number VS Coefficient of Discharge. It is believed that Reynolds Number shows positive results on the coefficient of discharge as depicted by the graph below.

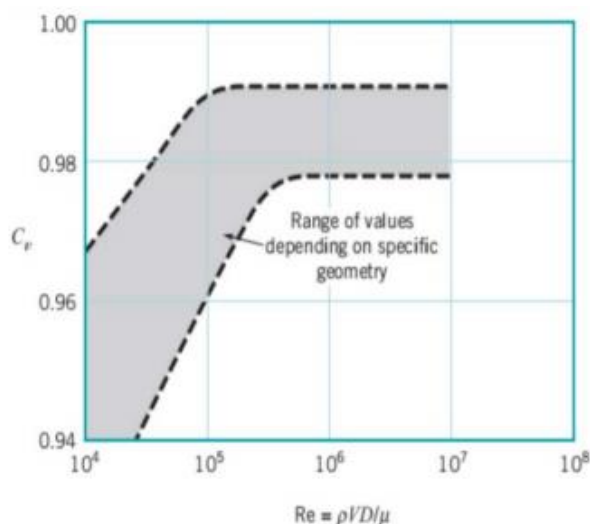


Figure 1.6 Idealised Re vs  $C_d$  curve

## 1.4 OBJECTIVES OF THE CURRENT STUDY

The essential goal for the investigation was to decide the ideal convergent angle required to limit the pressure drop for various Venturi structures with differing beta proportions. They are described elaborately below as:

- Find out the optimum Angle of Convergence for a standard ASME Venturi meters out of the given range of 19-22 degrees.

- Testing the  $\beta$  – ratios of 0.4, 0.5 and 0.6 for different angles of convergence and finding the ones yielding the best Coefficient of Discharge and the least pressure drop.
- Finding the variation of  $C_d$  at different Reynolds No. for each convergent angle.
- This research used CFD and also lab data (for  $\beta = 0.6$ ) to demonstrate the effect of the angles of the convergent cone on the coefficient of discharge on common Venturi meter designs.

## CHAPTER 2

### LITERATURE REVIEW

**B. Zachary et al. (2017)** in his work *Minimized Head Loss and ASME Venturi Recovery Cone Angle* is optimized. The paper referenced that Venturi stream meters are a reasonable alternative in numerous occasions where exceptionally exact stream flow estimation and low head loss are required. Its exactness for stream flow estimation is entrenched and archived; be that as it may, the structure of recovery cones and their related head loss isn't. To show the connection between recovery cone angle on the old style Venturi meter design and associated head loss, this examination utilized computational fluid elements and lab-centred information. Results demonstrated that, to limit head loss, the ideal recovery cone angle is an element of  $\beta$  ratio and Re. Though Venturi codes give scopes of adequate cone angles, this study gave the ideal RCA to limit permanent loss of pressure.

**R Arun et al., (2015)** in his paper "Prediction of Discharge Coefficient at low Reynold's number using Experimental and CFD method" studied, set up a computational model of a Venturi meter. This could be utilized as effective and simple methods for predicting the discharge coefficients at low Reynolds number. The computational Fluid Dynamics (CFD) programming ANSYS FLUENT-14 was utilized as a device to perform the modelling and recreation of Venturi meter. Analysis was completed for a standard Venturi meter and the outcomes were approved within the benchmarks. Further, the focal point of the investigation was coordinated towards stream flows with low Reynolds numbers regularly connected with pipe line transportation of viscous liquids. By considering the viscous losses that happen between two pressure taps, an analytical connection for discharge coefficient in the laminar region was inferred. The discharge coefficient diminishes quickly as the Reynolds number reduces. The outcomes were contrasted with the analytically proposed equation with  $C_d$  at low Re and furthermore



with the lab test information of Gordon Stobie. The outcomes acquired from every one of the three methods of estimations were with an uncertainty of 0.9 percent.

**Nithin T. et al. (2012)**, in their work “Optimization of Venturi Flow Meter Model for the Angle of Divergence with Minimal Pressure Drop by Computational Fluid Dynamics Method” uses the CFD software ANSYS FLUENT as a tool for modelling and simulation of the Venturi meter. The computation yielded that there is a minimum drop in pressure in the instrument only for one value of divergent cone for an unchanged convergent cone. The CFD results were matched with those of the results of Venturimeter installed at R V College of Engineering. For a better throat shape and the overall Venturimeter design the outcomes of this study can be used. Also, this can lead to a reduction in the cost of pumping in the system.

**Sudhakar K. (2017)** in the study “CFD analysis on different geometries of Venturi meter by using Fluent” analysed that the Venturi meter geometry is directly proportional to fluid flow parameters like pressure, velocity, and turbulence. In this project, analysis of 3 different geometries of Venturi meter is done by describing fluid flow parameters. Fluent software product of Ansys and computational fluid dynamics (CFD) principles were used for necessary numerical computations, analysis and to plot the parameters of the flow of fluid through the different geometries of the Venturi meter.

**Hollingshead C.H., et al. (2011)** in the work “Discharge coefficient performance of Venturi, standard concentric orifice plate, V-cone and wedge flow meters at low Reynolds numbers” The link between the Re and differential producer coefficient( $C_d$ ) was gotten through solutions for the steady, Reynolds-averaged Navier–Stokes conditions. To approve the numerical outcomes, discharge coefficients were additionally acquired tentatively through laboratory experiments. The focal point of the study was coordinated towards low Reynolds numbers generally concerns with pipeline transportation of fluids

with viscosity. Anyway high Reynolds number was additionally considered. It was inferred that, the discharge coefficients decline quickly at low values of Reynold's number with diminishing Reynolds number for Venturi, V-cone, and wedge stream meters. The orifice plate meter did not follow the general patterns of different meters, but instead the discharge coefficient expanded to a most extreme before strongly dropping off with further reduction in the Reynolds number as the Reynolds number diminished

**Tamhakar N., et al. (2014)** in his paper “Experimental and CFD analysis of flow through Venturi meter to determine the coefficient of discharge” studied and formed computational fluid dynamics model of a Venturi meter, so that instead of costly experimental methods, that CFD model can be effectively used. Along with studying the theoretical venturi aspects and using Bernoullie's equation for data calculation, this research analysed the experimental data and plotted graphs for the same. The study focuses on figuring out the pressure differential across the Venturimeter section. This is done by means of Fluent 13.0 which an ANSYS tool is exploring the use of CFD methods to find out the parameters of flow in the venturi meter. This research compared the results calculated by both, the CFD and experimental methods. This is carried out to validate Bernoulli's equation when applied to the steady flow of fluids in a tapered duct and to calibrate the Venturimeter as a flow-meter by analysing and finding the coefficient of discharge

**Ameresh H. , et al. (2017)** in his work “ Investigation of Mass Flow Rate in Venturi meter Using CFD Analysis “ analysed varying firth/inlet diameter of Venturi meter such as 25mm, 30mm and 35mm. For mass flow rate of air, theoretical calculations were done. FLUENT values and theoretical values were compared. Using the variation of the inlet pressure, the mass flow rates of  $Al_2O_3$ , air and water passing through different diameters of Venturi meter were calculated. For modelling of Venturi meters with inlet diameters of 25 mm, 30mm and 35mm, a software named as Unigraphics was used. For finding out

the values of the mass flow rate values for Venturimeters, Finite Element Analysis software ANSYS FLUENT is utilized.

**Akapan P. (2014)**, in his research “A CFD simulation of water flow through a variable area Venturi Meter” used the Ansys fluent CFD tool, the pressure difference which is exerted on a bluff body object and calculated the flow field from inlet to outlet portion. This research studies the stream field from inlet to outlet, to explore the pressure distinction applied 25mm upstream and 25mm downstream of the bluff body object for various volumetric streamflow rates (4 l/s, 5 l/s and 8 l/s). The complete pressure loss over the plate for the 4 l/s, 5 l/s and 8 l/s streams were discovered 17.38 kPa, 27.14 kPa and 69.62 kPa separately due to the degree of turbulence with the 8 l/s stream having the greatest turbulence intensity of more than 250% surpassing those of the 4l/s and 5l/s streams which are ~130% and ~160% separately

**Sanghani H.R. et al. (2016)** in their study “Effect of Geometrical Parameters of Venturi meter on Pressure Drop” used CFD tool for investigating the effect of different parameter (mainly geometric) like angle of divergence,  $\beta$  ratio and length of the throat on pressure drop in Venturi meter. Effect of each parameter has been carefully computed, angle of recovery and also the length of throat while it reduces with increase in diameter re-checked by varying one parameter and keeping the other 3 constant at a time. It was found that with increase in the ratio of convergent cone angle pressure drop fluctuates.

**Harris M.J. et al. (2001)** in the paper “Discharge coefficients of Venturi tubes with standard and non-standard convergent angles” described 21 Venturi tubes manufactured for  $\beta$  ratio ranging from 0.4 - 0.75. Out of all the Venturis, standard are fifteen, having a converging cone angle of  $21^\circ$ , made in a range of pipe dia. from 50-200 mm and for  $\beta$  ratios from 0.4 - 0.75. Six are standard with the exception of the converging angles which are either  $10.5^\circ$  or  $31.5^\circ$ ; they are of dia. across 100 mm. The calibration for all of the Venturis is done in high pressure gas and water. For the standard Venturi tubes a condition

for the coefficient of discharge in water has been acquired with an uncertainty of 0.74 percent. Work on the physical premise of the equation for the coefficient of discharge at high  $Re$  is portrayed, and a fitting equation for every one of the gas information from the standard Venturi meters with an uncertainty of 1.23 percent is inferred. Unmistakably the information in gas from the Venturis having converging cone of  $10.5^\circ$  is much smoother than that from Venturi meters with the standard or the higher united edge: a condition fitting every one of the gas information from the three Venturi tubes with a joined edge of  $10.5^\circ$  has been gotten with a uncertainty of 0.71 percent

## CHAPTER 3

### METHODOLOGY

For this study, the development of Numerical model and lab experimentation was done at the Delhi Technological University Laboratory. The primary computer that was used for computer model development, was a HP 3230M which has the following specifications: 8 GB Random Access Memory (RAM), an i5, 2.60Ghz processor with an operating system of 64 bits, 1 TB ROM, and a Windows 8.1 system. The physical models were developed in ANSYS SPACECLAIM, then exported to FLUENT 18.1 for meshing and analysis. Every model was modelled and developed in Space Claim Design Modeller, with X-Y as the plane of geometry. The geometry of the lab-tested Venturi was designed to duplicate its drawing.

The laboratory testing done was done on the Venturi Model available in the lab. The Venturi model in the lab has a  $\beta$ -ratio of 0.6. The Venturi equipment has two different pipe dimensions with one pipe of inlet pipe diameter as 20mm and the other as 35mm. The pipe material was Galvanised Iron. A collection tank installed at the outlet with an area of 200 mm<sup>2</sup> was used for the discharge measurement.

#### 3.1 PROCEDURE: ANSYS FLUENT

The first step included the construction of model geometry in SCDM, after which meshing of models was done to find out the points within the geometry where numerical computations will take place. After a test of multiple schemes in mesh, it was concluded that the optimum size function would be curvature so as to capture the conical transitions in Venturi geometry, while keeping the element size as 0.003m. The mesh was even made finer by introducing refinement of the mesh for different elements in geometry. After the completion of model meshing, there were up to 500000 computational elements/computational nodes in the model.

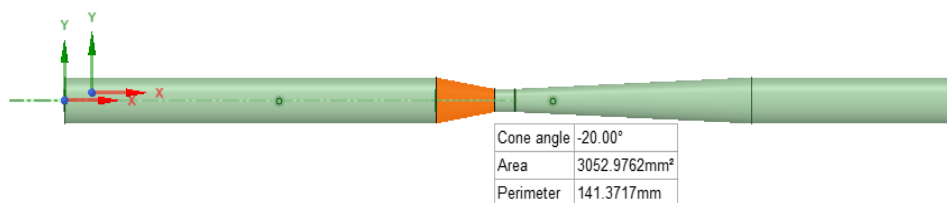


Figure 3.1 Geometry in SCDM

One of the most important processes for model created in Space Claim design modeller is defining the boundary conditions. The name velocity inlet is given to the flow inlet on the 30mm dia. u/s pipe. The outlet was defined as the exit pipe of the venturi meter. The other faces in the constructed geometry are all identified as walls. In order to compare the measured flow data from the laboratory data, the velocity inlet boundary condition is used. By giving outlet condition for pressure it is ensured that with different fixed outlet pressures the differential pressure through the venturimeter should be unaltered. After adding the boundary limitations to different faces of the SCDM model, the other specifications were added in the FLUENT software.

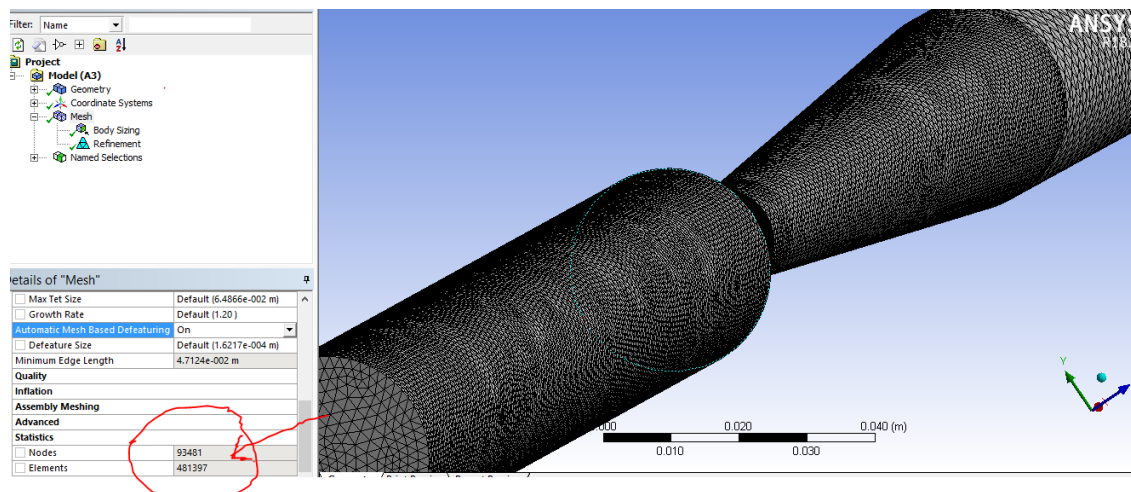


Figure 3.2 Figure depicting nodes and elements in a mesh

FLUENT was then used and the case file for the mesh was read. The tet/hybrid cells shown in Figure 3.2 were converted to polyhedral cells to significantly reduce computation time normally associated with hybrid cells. Through the completion of many test runs it was found that the best viscous turbulence models for this study were the standard or the realizable k-epsilon models. However, for this study Standard K-epsilon was used as the difference between the two was meagre. This particular model

was used for all the runs that had a Reynolds number greater than 2,000. All the constants associated with this version of FLUENT were set to their default values unless otherwise specified. Under the materials tab in FLUENT, the fluid was changed to water/liquid and the solid material by default was kept as Aluminium. The boundary conditions for velocity at inlet are kept as 1 m/s, corresponding to the Reynolds Number value of around 33500. The pressure Outlet was kept so as to have the gauge pressure at that point equal to zero.

In this research, the Simple Consistent algorithm as the pressure velocity coupling has been used. The Under-Relaxation Factor had been set to the standard FLUENT values ranging from 1 to 0.7 for all of the variables except the pressure factor, which for this study was set to 0.3. The Second Order Upwind method was used for momentum and first order upwind scheme for kinetic energy, and the turbulent dissipation rate only for this study along with the standard pressure were used. The convergence of a solution such that a point is reached where there is a little difference between the successive iterations was done with the help of residual monitors. For the standard k-epsilon model use here, 6 different residuals were monitored which had the following inclusions: continuity, x, y, and z velocities, k, and epsilon. The utmost iterative accuracy in this study is achieved by requiring the residuals to converge to 0.001, before the run of each model was complete.

The models were initialized with hybrid initialization as the main initialization schemes along-with the velocity input, just to make sure that the trials performed initially gave credible outcomes. While initializing, at least 100 iterations were done on the software while plotting the residuals and monitoring any unusual increments. Most of the solutions converged within these iterations. As the iterations converge, the initial results are checked to ensure that all boundary limitations perform correctly and other obvious errors are not present.

Surface planes, aligned to X-Y plane are created for determination of resultant pressure at pressure tap locations for each of the Venturi meters. Surface plane, as shown in Figure 3.3 is a cross-sectional view, depicting pressure at both of the pressure taps location. The values of pressures obtained at the two tap locations were used to compute

the values of discharges which was then compared with the theoretical values of discharge to obtain an estimation of Coefficient of Discharge.

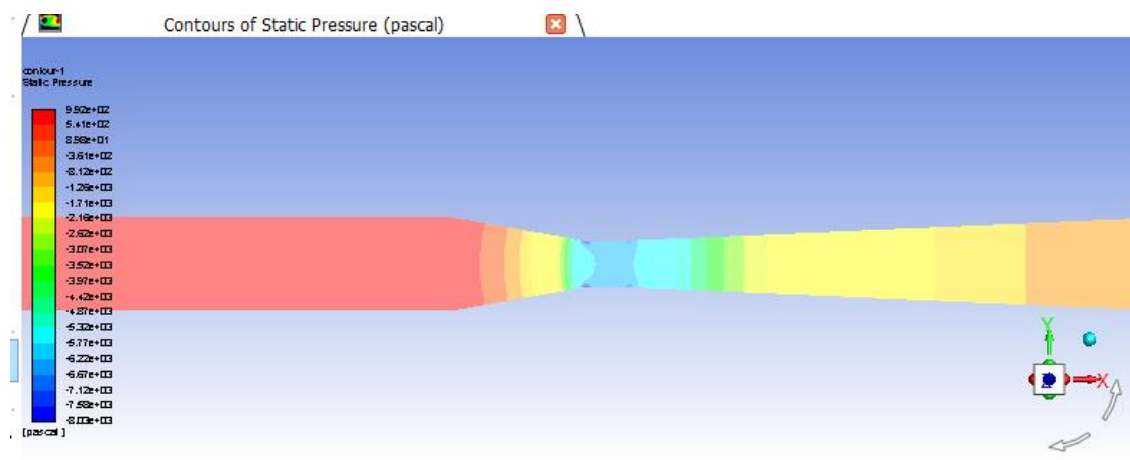


Figure 3.3 A surface plane depicting static pressure contour

To notice the effect of Reynolds number on the convergent angle, 3 Reynolds number were selected and each convergent angle was tested for those three Re value.

### 3.2 PROCEDURE: LAB

The lab arrangement had two set of pipes with a common collection tank. The two types of pipe had control valves for the adjustment of discharge. The procedure includes measurement of head difference as observed in the manometer legs and then convert it into discharge with the help of equation, as given in the introduction section. This is known as the  $Q_{\text{theoretical}}$ . The other value that is  $Q_{\text{actual}}$  is found with the help of volume in the collection tank divided by time taken to fill that volume. The ratio of these values, gives the value of  $C_d$ .





**Figure 3.5** Laboratory arrangement for the two Venturi meters



**Figure 3.6** Collection tank of the Venturi meter

## CHAPTER 4

### RESULTS AND DISCUSSIONS

As the study included both laboratory and computational experiments, results were found out for both after following the methodology followed in section 3. Both the results were in form of pressure drops between the two pressure taps in the Venturi meter. The head difference thus obtained had to be further analysed in order to obtain theoretical as well as actual discharge values. These discharge values for further used to obtain the coefficient of discharge. For that analysis, formulas were mentioned in the introduction section. This section presents those values and the calculations as well.

#### 4.1 ANSYS FLUENT RESULTS

The ANSYS computations were done for 3  $\beta$  – ratios (0.4, 0.5 & 0.6). For each  $\beta$ -ratio, 21 models, corresponding to different convergent cone angle and variable Reynolds Number were made.

As given earlier, the value of Coefficient of discharge is given as:

$$C_d = \frac{Q_{th}}{Q_{act}}$$

The  $Q_{theoretical}$  is computed by simply multiplying the value of area of input pipe with the input velocity. For this study, a standard 30 mm pipe has been taken.

$$\text{Area of the inlet pipe/ Area at the upstream tap} = A_1 = 7.06858 * 10^{-4} \text{ m}^2$$

The computation of theoretical discharge is done with the help of the input velocity (entered value in the ANSYS) which in turn affects the Reynolds Number. This implies that different input velocities have different Reynolds number and therefore different theoretical discharge values.

$$Q_{th} = A_1 * V_1$$

Table 4.8 Theoretical Discharge values at different velocities

$\beta$ -ratio	Input ANSYS velocity, $V_1$ (m/s)	Inlet Reynolds Number	$Q$ theoretical ( $m^3/s$ )
0.4,0.5,0.6	0.2966	10000	$2.0964 * 10^{-4}$
	1	34000	$7.06858 * 10^{-4}$
	2.966	100000	$2.0964 * 10^{-3}$

#### 4.1.1 $\beta$ ratio = 0.4

It is necessary to understand that the value of actual discharge will differ for every  $\beta$  – ratio. Different ratios imply different entry lengths and therefore difference in turbulence and also increase/decrease in frictional losses. These losses are visible in terms of difference in pressure drops for different  $\beta$  values. For the computation of the  $Q$  actual, the pressure difference at the pressure taps, obtained by the pressure plane constructed on Fluent is used in equation 1.1 to compute the discharge.

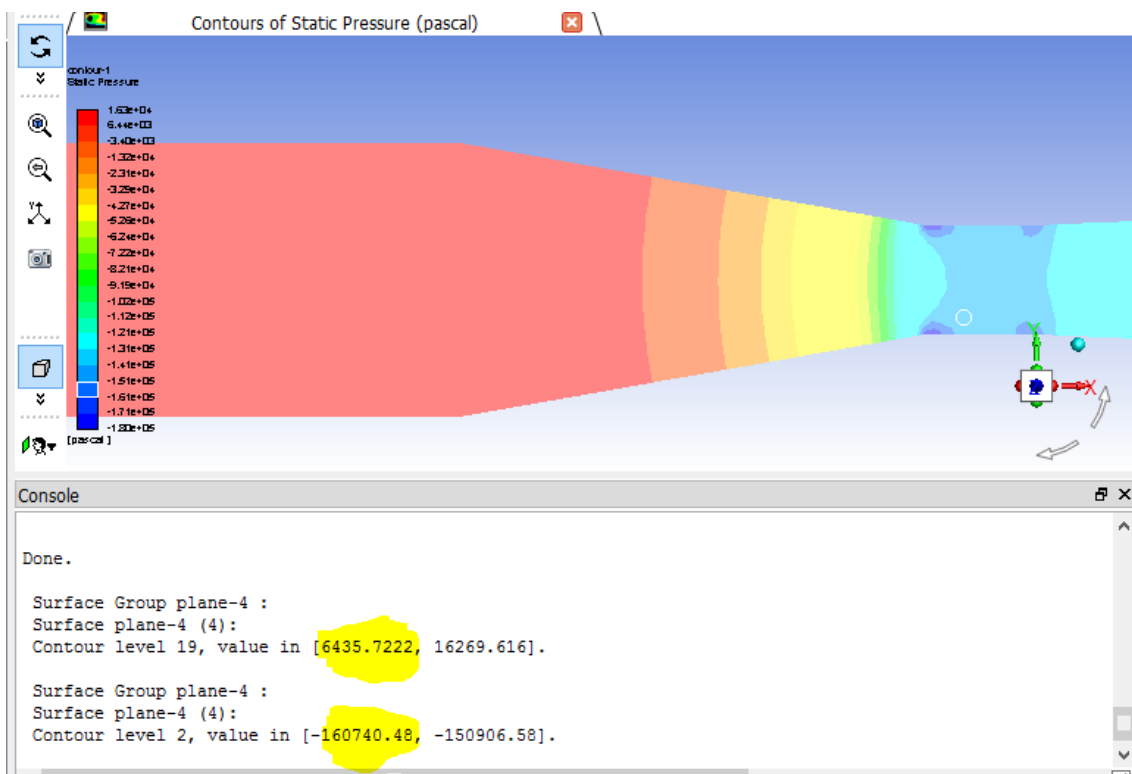


Figure 4.1 Pressure at two pressure taps

The values highlighted in Figure 4.1, shows the pressure at two tap locations of the Venturi. These values are then used to compute the  $Q_{act}$ , which is in turn used to compute the coefficient of discharge as shown in table 4.2. The value in the table below are only corresponding to the inlet Reynolds number of around 34000.

**Table 4.9  $C_d$  for different converging angles of  $\beta$  ratio = 0.4**

Convergent Angle	$\Delta p$ (Fluent Value) (Pa)	Corresponding $Q_{act}$	$C_d$
19	19881.9813	0.0723563	0.9769
19.5	19186.910	0.071078	0.9974
20	19076.4588	0.0708740	0.9943
20.5	19231.5325	0.07116153	0.9933
21	19213.5295	0.0712089	0.9926
21.5	19336.4099	0.0713553	0.9906
22	19337.2105	0.07135678	0.9905

These values can be shown graphically, as done in figure 4.2. The graph can be used to find the angle corresponding to the maximum  $C_d$ .

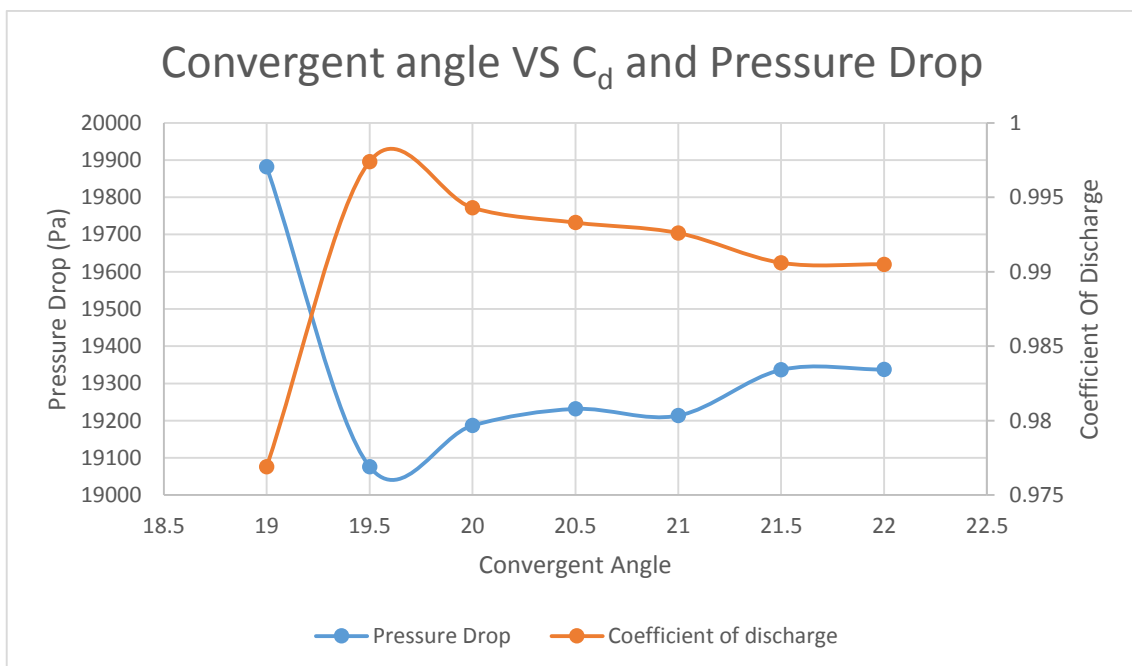


**Figure 4.2 Graph showing the optimum Convergent angle for  $\beta = 0.4$**

The graph corresponding to inlet Reynolds number of 34000, shows that the value corresponding to the convergent angle of 20 degrees yields the least value of pressure drop or the best value of Coefficient Of Discharge i.e. 0.9973. Table 4.3 and Figure 4.3, shows a detailed graph for all the values of convergent angle at all the Reynolds number under consideration.

It is necessary to note that on controlling the convergent angle, 4% of the loss in terms of pressure can be avoided, as given by the pressure drop values given in Table 4.2.

**Table 4.10  $C_d$  for different Reynolds Number for  $\beta = 0.4$**

<b>Convergent angle</b>	<b>Reynolds Number</b>	<b>Coefficient of discharge</b>
19	10000	0.9721
	34000	0.9769
	100000	0.9787
19.5	10000	0.9887
	34000	0.9964
	100000	0.9993
20	10000	0.9925
	34000	0.9963
	100000	0.9972
20.5	10000	0.9901
	34000	0.9933
	100000	0.9951
21	10000	0.9898
	34000	0.9926
	100000	0.995
21.5	10000	0.9881
	34000	0.99
	100000	0.9911
22	10000	0.9897
	34000	0.9905
	100000	0.9935

The above table shows the variation of the  $C_d$  over a range of Reynolds number, it even solidifies the fact that 19.5 degrees is the optimum angle for  $\beta = 0.4$  as on increasing the Reynolds number further for that CA, the  $C_d$  value further increases.

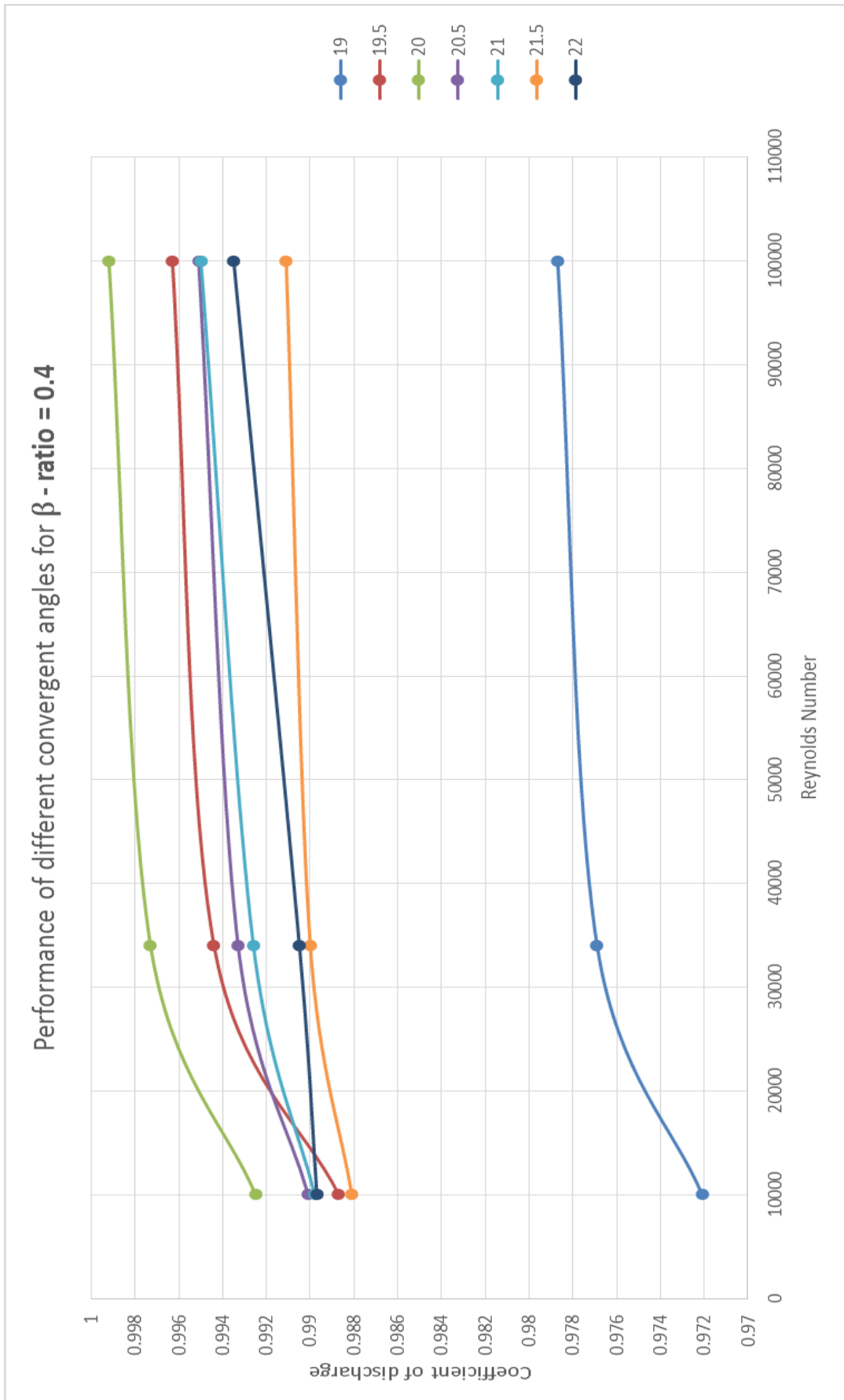


Figure 4.3 Graphical representation of coefficient of discharge for different Reynolds Number and Convergent Angle for  $\beta = 0.4$

### 4.1.2 $\beta$ – ratio = 0.5

The above mentioned procedure for computation of  $C_d$  is repeated for this value of  $\beta$ .

**Table 4.11  $C_d$  for different converging angles of  $\beta$  ratio = 0.5**

Convergent Angle	$\Delta p$ (Fluent Value) (Pa)	Corresponding $Q_{act}$	$C_d$
19	7639.2953	0.07142	0.9896
19.5	7606.3997	0.07777	0.9917
20	7664.8414	0.071546	0.9879
20.5	7782.9383	0.072095	0.9804
21	7763.7068	0.072006	0.9816
21.5	7747.55301	0.0719312	0.9826
22	7787.16984	0.072114	0.9801

Surprisingly, the optimum value for this  $\beta$  occurs at 19.5°, which is ideally out of the range of ASME limits but was tested for the this study. This can be made out by the graph in Figure 4.4.

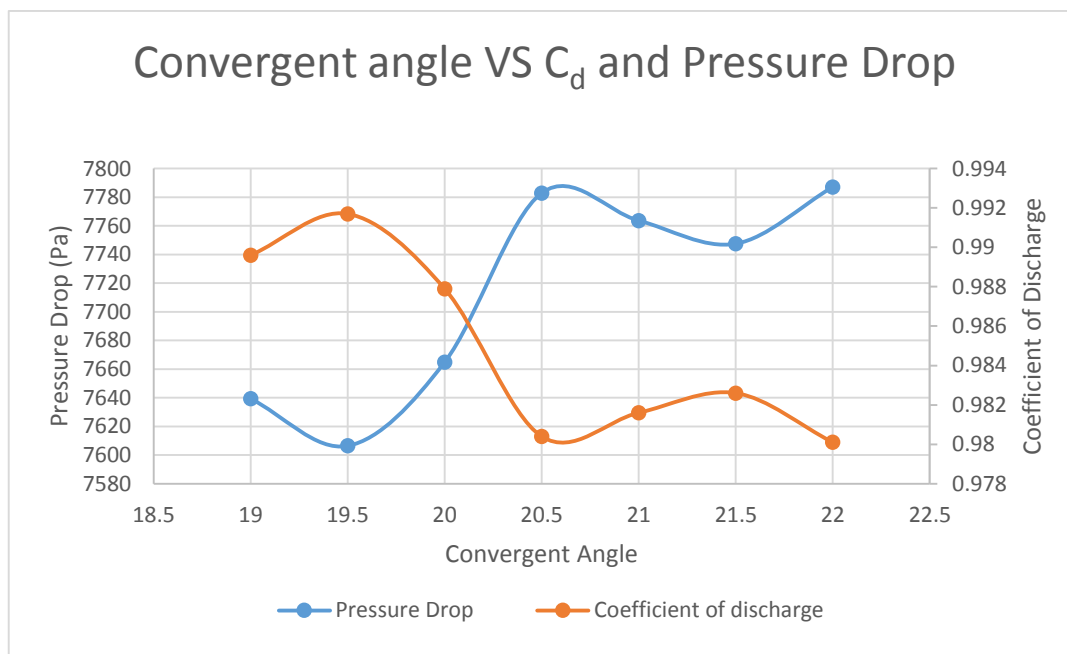


**Figure 4.4 Graph showing the optimum Convergent angle for  $\beta = 0.5$**

The Reynolds Number and variation associated with it for  $\beta = 0.5$  is depicted in Table 4.5. The trend stays the same here, with increase in the Reynolds Number value corresponding Coefficient of discharge also increases.

Table 4.12  $C_d$  for different Reynolds Number for  $\beta = 0.5$ 

Convergent angle	Reynolds Number	Coefficient of discharge
19	10000	0.98
	34000	0.9896
	100000	0.9899
19.5	10000	0.9901
	34000	0.9917
	100000	0.9936
20	10000	0.9822
	34000	0.9879
	100000	0.9896
20.5	10000	0.9796
	34000	0.9804
	100000	0.9896
21	10000	0.9801
	34000	0.9816
	100000	0.9888
21.5	10000	0.9799
	34000	0.9826
	100000	0.9899
22	10000	0.9763
	34000	0.9822
	100000	0.9888

The graphical representation of the data in Table 4.12 can be seen from Figure 4.5. The value of the maximum CA can be observed by these curves.



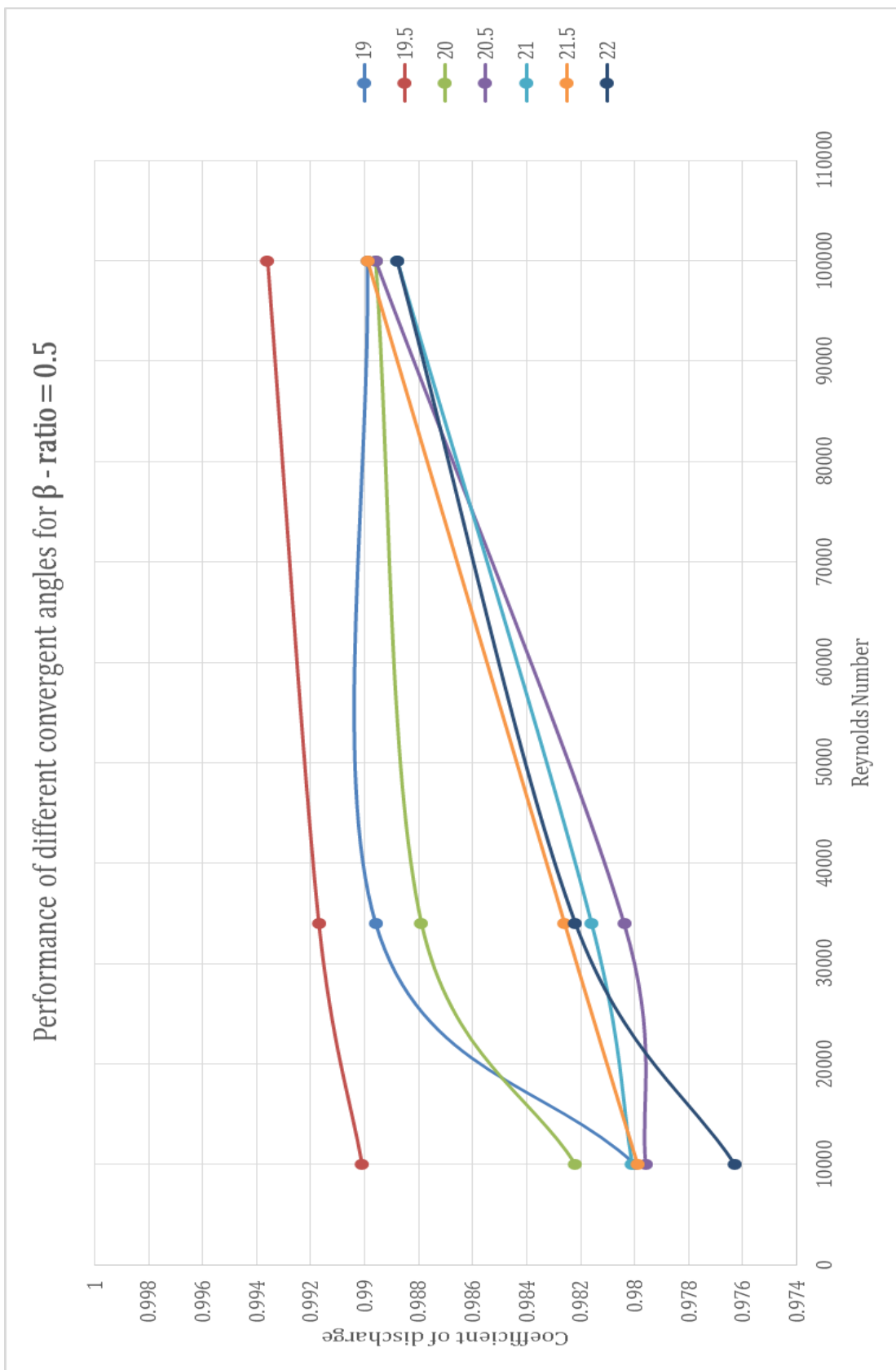


Figure 4.5 Graphical representation of coefficient of discharge for different Reynolds Number and Convergent Angle for  $\beta = 0.5$

### 4.1.3 $\beta$ – ratio = 0.6

As discussed above, the computations for this ratio is also done in the very same manner.  $C_d$  shows a huge variation for different CA's. Table 4.6 shows the variation and the pressure drop as well.

**Table 4.13  $C_d$  for different converging angles of  $\beta$  ratio = 0.6**

Convergent Angle	$\Delta p$ (Fluent Value)	Corresponding $Q_{act}$	$C_d$
19	3511.60513	0.0723103	0.97753
19.5	3560.33215	0.0728931	0.96967
20	3563.11174	0.0729216	0.96930
20.5	3381.03648	0.0710340	0.99509
21	3397.6590	0.0712084	0.9926
21.5	3393.02758	0.071159	0.99337
22	3415.7200	0.0713974	0.99030

This is the highest ratio to be tested in this study. The optimum value of CA in this case lies well within the range specified by ASME. The Optimum convergent cone angle comes out to be  $20.5^\circ$ , with the  $C_d$  value of 0.995 as shown in Figure 4.6.

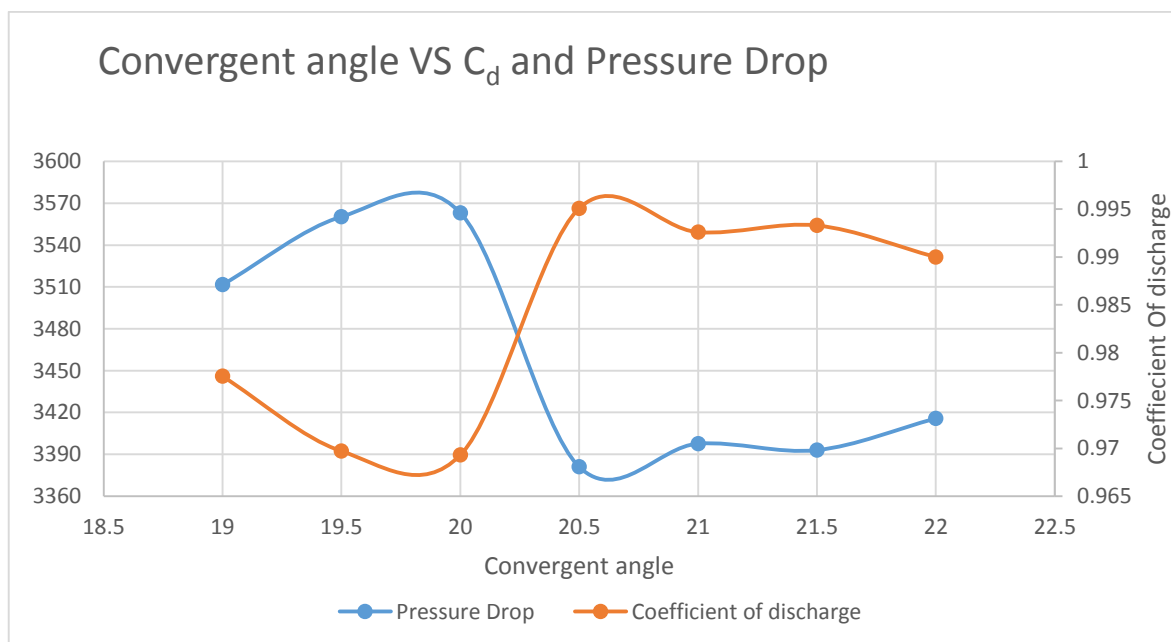


**Figure 4.6 Graph showing the optimum Convergent angle for  $\beta = 0.6$**

The effect of Re on  $C_d$  is computed and shown in Table 4.7 and graphically for different Convergent angles in Figure 4.7.

Table 4.14  $C_d$  for different Reynolds Number for  $\beta = 0.6$ 

Convergent angle	Reynolds Number	Coefficient of discharge
19	10000	0.9701
	34000	0.9775
	100000	0.981
19.5	10000	0.9676
	34000	0.9697
	100000	0.9716
20	10000	0.9633
	34000	0.9693
	100000	0.9723
20.5	10000	0.9928
	34000	0.995
	100000	0.9972
21	10000	0.9901
	34000	0.9926
	100000	0.9963
21.5	10000	0.9907
	34000	0.9933
	100000	0.9954
22	10000	0.9889
	34000	0.99
	100000	0.991

Figure 4.7 below shows the graphical form of data in the Table 4.14. It solidifies the fact that 20.5 degrees is the optimum CA.

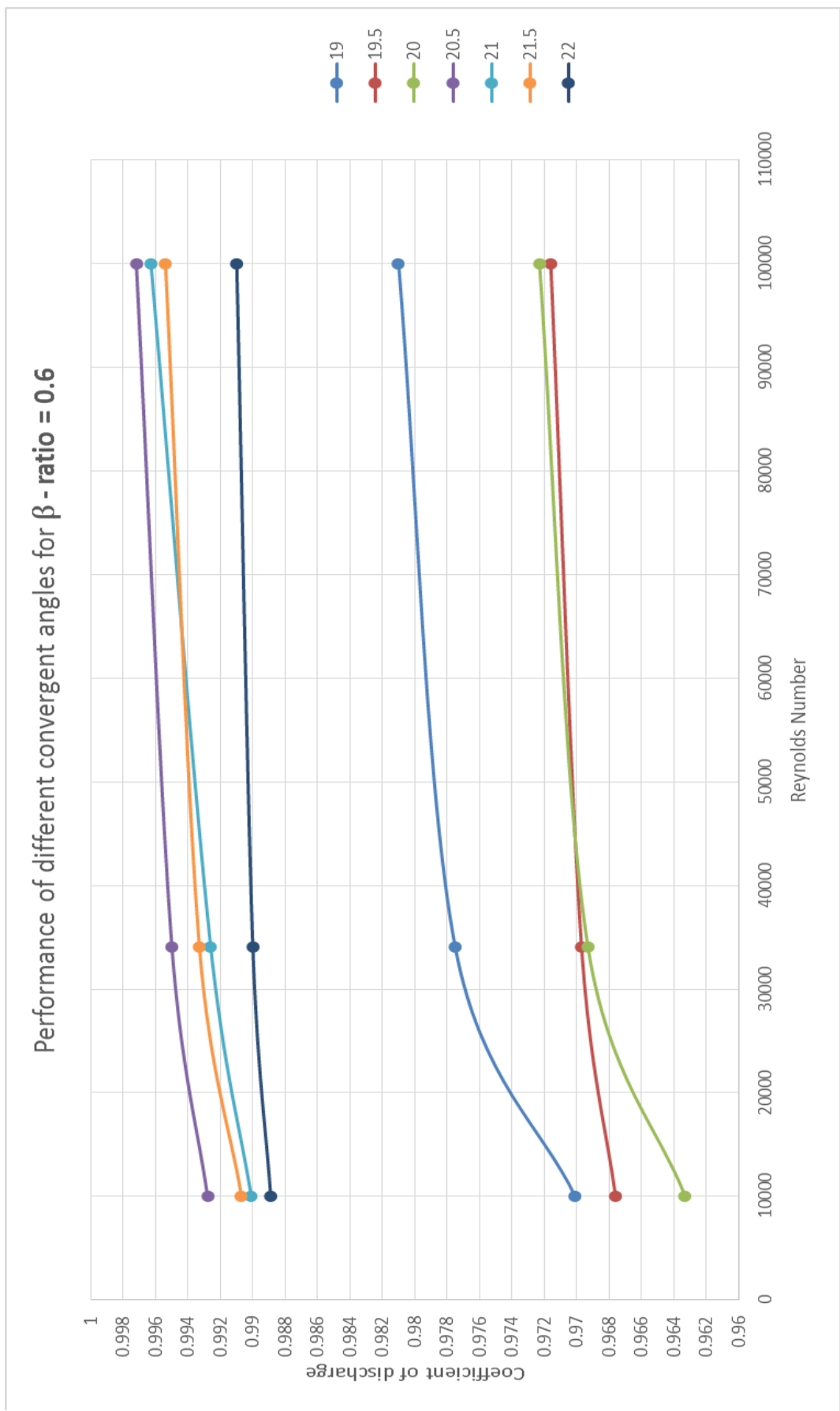


Figure 4.7 Graphical representation of coefficient of discharge for different Reynolds Number and Convergent Angle for  $\beta = 0.6$

## 4.2 LABORATORY RESULTS

As mentioned earlier, the Venturimeters present in the DTU lab have a  $\beta$  ratio of 0.6. Therefore, this section shows the comparison of lab results for 0.6  $\beta$  ratio with the CFD results as presented in section 4.1.3. As the convergent angle in the lab is constant, the comparison shown is for an inlet convergent angle of  $21^\circ$ , with a Recovery cone angle of  $5^\circ$ . The parameter varied here is Reynolds Number only.

**Table 4.15 Experimental results for  $\beta = 0.6$**

Inlet Pipe Size, mm	Manometer Reading		$\Delta h$ of water (m)	Discharge ( $m^3/s$ ) $Q_{th}$	Discharge ( $m^3/s$ ) $Q_{act}$	Reynolds Number, Re	$C_d$
	Left Limb (cm)	Right Limb (cm)					
35	27.1	25.2	0.239	$8.04 \cdot 10^{-4}$	$9.06 \cdot 10^{-4}$	37032	0.888
	28.3	24	0.541	$1.21 \cdot 10^{-3}$	$1.30 \cdot 10^{-3}$	53406	0.926
	29.6	22.5	0.894	$1.53 \cdot 10^{-3}$	$1.55 \cdot 10^{-3}$	62667	0.985
	30.8	19.6	1.411	$1.97 \cdot 10^{-3}$	$1.98 \cdot 10^{-3}$	80661	0.989
20	10.6	9.8	0.108	$1.76 \cdot 10^{-4}$	$2.25 \cdot 10^{-4}$	16087	0.782
	11	9.4	0.217	$2.50 \cdot 10^{-4}$	$3.08 \cdot 10^{-4}$	22078	0.811
	11.5	8.8	0.367	$3.35 \cdot 10^{-4}$	$4.01 \cdot 10^{-3}$	29287	0.835
	16.5	4.0	1.706	$7.01 \cdot 10^{-4}$	$7.61 \cdot 10^{-3}$	54386	0.921

The laboratory tests is limited to a range of Reynolds Number as discharge can only be increased to a certain extent. Therefore, the range is limited. Table 4.15 indicates all the values, including values of  $C_d$  as well. A sample of how calculation is done is shown below.

Considering the first reading, head in terms of cms of mercury:

$$27.1 - 25.2 = 1.9 \text{ cm}$$

In terms of head of water,  $\Delta h$ :  $1.9 * 12.6 = 23.94 \text{ cm} = 0.2394 \text{ m}$  of water

Area of inlet pipe,  $a_1 = 9.6211 * 10^{-4}$

Area for throat section of first pipe (corresponding to diameter of 21mm),

$$a_2 = 3.14 * 10^{-4}$$

Consider Equation 1.1

$$Q_{theoretical} = C_d \frac{a_1 a_2}{\sqrt{a_1^2 - a_2^2}} \sqrt{2gh}$$

$$\frac{a_1 a_2}{\sqrt{a_1^2 - a_2^2}} \sqrt{2g\Delta h} = 8.04 * 10^{-4} \text{ m}^3/\text{s}$$

Difference in elevation level of collection tank having dimensions 0.4m \* 0.5m in 30 seconds = 15.5 – 8.7 = 6.8 = 0.068m

Volume of liquid in 30 seconds = 0.068 \* 0.5 \* 0.4 = 0.0136 m<sup>3</sup>

Actual discharge,  $Q_{actual} = 9.0667 * 10^{-4} \text{ m}^3/\text{s}$

Coefficient of discharge,  $C_d = \frac{8.04 * 10^{-4}}{9.0667 * 10^{-4}} = 0.888$

The values of  $C_d$  against Reynolds Number given in table 4.8 are plotted in Figure 4.8. It gives a comparison of CFD and lab results. It is observed that lab results vary a little from the CFD curve. It is because the CFD computations took smooth wall under consideration, whereas the lab conditions vary a little. But, in any case it is safe to say that the change in  $C_d$  is comparable in both the cases. It can be observed through the graph, that in the range of study, that is, for Reynolds number 20,000 – 100,000, the coefficient of discharge is observed to increase.

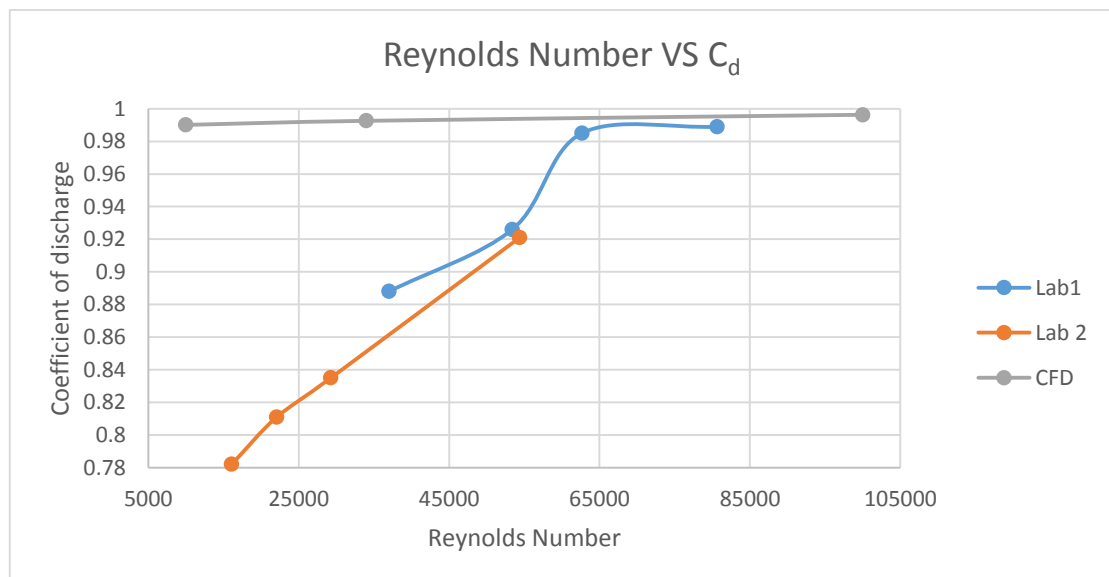


Figure 4.8 Plot comparing lab and CFD results

## CHAPTER 5

### CONCLUSIONS AND DISCUSSIONS

This research uses physical and numerical data for determining optimum CAs for different Venturimeter designs. Three different  $\beta$  ratios of 0.40, 0.50, and 0.60 were analysed with constant wall roughness, three different Re's and multiple CAs. The points mentioned below describe the findings of this research.

- CFD has the ability to produce data that can predict pressure loss/drop for different designs of Venturimeter. Through this study it is observed that the convergent angle corresponding to the maximum coefficient of discharge also has the least value of pressure drop. Therefore, it is necessary to design the Venturi meters of the  $\beta$  ratios under consideration to be manufactured/ constructed as per the convergent angle reflected in this study. This will prevent the pressure loss and help in discharge estimation with error less than 0.25%. The table below gives the % loss in pressure, which can be avoided if the optimum CA's as pointed in this research, are used. These tables are collectively derived from pressure drop values from table 4.2, 4.4 and 4.6.

**Table 5.1 Loss in different ratios**

$\beta$ ratio	% loss of pressure that can be avoided by providing optimum CA
0.4	4.051
0.5	2.380
0.6	5.110

Therefore, it is inferred that measurement for head loss are sensitive to the angle of convergence. It is implied that small variations in the angle of convergence can lead to considerable increase/decrease in pressure.

- The Convergent angles are proved to be a function of  $\beta$  ratio and Reynolds Number. The best CA angle corresponding to each  $\beta$  ratio as found is given in table 4.10.

Though the analysis shows an increasing trend of convergent angle with increase in  $\beta$  – ratio, more rigorous research has to be done to establish a proper relationship between the two.

**Table 5.2 Optimum CA corresponding to different  $\beta$  ratio**

$\beta$ ratio	Optimum CA
0.4	19.5°
0.5	19.5°
0.6	20.5°

- To validate the results obtained by CFD, an equation presented by M.J Reader Harris as in reference [6], is used.

$$C_{water} = 0.9878 + 0.0123\beta \quad (4.1)$$

This equation is used is used to relate  $C_{water}$ , that is, the coefficient of discharge of a Venturi tube, having water as the flowing fluid with  $\beta$ . This equation has an uncertainty of 0.74% (based on two standard deviations). To check the results, the value of  $C_d$  obtained by at optimum CA's were compared with the  $C_{water}$ . The error percentage is calculated and checked that if it is within the limit.

**Table 5.3 Validation of the CFD results**

$\beta$ ratio	Computed $C_d$	$C_{water}$ from Equation 4.1	% error
0.4	0.9974	0.9927	0.46
0.5	0.9917	0.9939	0.22
0.6	0.9950	0.9951	0.018

It is seen that error is even less than 1%, therefore the result is very well validated.



- The relationship between Reynolds number and  $C_d$  is also very well established here with the help of CFD results validated through the lab results. The curve obtained through both the data are seen to follow a rising trend. The trend signifies that on increasing the Reynolds Number (within the experimental range), the  $C_d$  also increases.

## REFERENCES

- [1] B. Zachary, J. Michael and B. Steven, "Optimizing the ASME Venturi Recovery Cone Angle to Minimize Head Loss", ASCE, *J. Hydraul. Eng.*, 144(1): 04017057, (2017)
- [2] H. Ameresh, P. Ravikanth and DepaSandeep, et al. "Investigation of Mass Flow Rate in Venturimeter Using CFD Analysis", ISSN : 2248-9622, Vol. 7, Issue 12, ( Part - 7) December 2017, pp.86-90, (2017)
- [3] Tamhakar N. and A. Pandhare, "Experimental and CFD analysis of flow through venturimeter to determine the coefficient of discharge", Vol. 3, Issue 4, March 2014
- [4] Nithin T. et al. (2012), "Optimization of Venturi Flow Meter Model for the Angle of Divergence with Minimal Pressure Drop by Computational Fluid Dynamics Method", International Conference on Challenges and Opportunities in Mechanical Engineering, Industrial Engineering and Management Studies 658 (ICCOMIM - 2012), 11-13 July, 2012
- [5] Hollingshead C.L. and M.C. Johnson "Discharge coefficient performance of Venturi, standard concentric orifice plate, V-cone and wedge flow meters at low Reynolds numbers", *Journ. Of Petroleum Science and Engineering* 78 (2011), pp 559-566.
- [6] Harris M.J. and W.C. Burton, "Discharge coefficients of Venturi tubes with standard and non-standard convergent angles", ASCE, *Flow Measurement and Instrumentation* 12, (2001), pp 135-145
- [7] ASME MFC-3M-2004, "Measurement of Fluid Flow in pipes using Orifice, Nozzle and Venturi", Part 4, pp 68-83 (2004).
- [8] K. Sudhakar, "CFD Analysis on different geometries of Venturimeter by using FLUENT", *Indian journal of Research*, Volume 6, Issue 7, July 2017
- [9] Akapan P. and P. Udeme, "A CFD simulation of water flow through a variable area Venturimeter", *International Journal of Current Research*, Vol 6, Issue 03, pp 5425-5431, March 2014